AZPH-TH/95-21

Resolved Photon and Rapidity Gap in Jet Events *

Hung Jung Lu

Department of Physics, University of Arizona

Tucson, AZ 85721

(February 1, 2008)

Abstract

We study the production of jet events containing large rapidity gaps in particle colliders due to the resolved photon mechanism. In particular, we analize these events at DESY HERA and future e^+e^- linear colliders, including the possibility of $\gamma\gamma$ laser backscattering beams. These events allow the study of the perturbative pomeron in environments complementary to the hadron-hadron colliders, and also provide insight into the survival probability of the rapidity gaps involving photon initial state.

12.38.-t, 13.60.-r, 13.65.+i, 13.85.-t

Typeset using REVTEX

*Work supported by the Department of Energy, contract DE–FG03–93ER–40792.

I. INTRODUCTION

The energy range of present and future particle colliders opens a kinematic regime, where the observation of jet events containing large rapidity gaps can provide interesting physical insight into the underlying exchange mechanisms. The presence of rapidity gaps can also serve as triggering signal in high-mass scale physics [1–3]. Events containing large rapidity gaps have recently been observed at hadron-hadron collider [4] and lepton-hadron collider [5,6]. However, the possibility of observing jets separated by large gaps is not limited to hadron-hadron or lepton-hadron colliders. In fact, lepton-lepton collisions can also generate these events [7,8]. Purely leptonic collisions provide an environment free of spectator interactions, and can give interesting complementary information to the rapidity gap physics of hadronic collisions.

Photon initiated collisions should provide yet another environment for the observation of jet events with rapidity gaps. The initial photons could be either real (for instance, by using a laser-backscattering beams [9]), or quasi-real, as those produced in the photoproduction events in ep and e^+e^-colliders via the Weisäcker-Williams equivalent photon mechanism [10]. In fact, in the DESY HERA case, the gap events occur both at the deep-inelastic regime [5] as well as the photoproduction regime [6]. (See also the theoretical models in Ref. [11].) However, at the moment the experimental situation has focused on the low $|t|$ region, where the proton or its low-mass excited state (like a Δ) propagates in the forward direction, escaping detection. In this paper we explore into the higher $|t|$ region, where the proton is broken and a hard jet with $p_T^2 \sim |t| \gg 1$ GeV^2 is generated from the broken proton. This corresponds to the double diffractive dissociation of the γp system.

From the study of resolved photon processes [12–14] (for a review, see Ref. [15]), we know that for the generation of jet events with fragments in forward and backward beam direction, the initial lepton can themselves be treated as containing hadronic components. Thus, one can talk about quark and gluon contents of electrons. For these jet events, the initial leptons would behave like supplier of the partons for the hard subprocess, much like

the initial hadrons in hadron-hadron colliders.

It is well known [16] that as the collision energy $\sqrt{s}$ increases, the cross section for the annihilation events at lepton colliders decreases like $1/s$ or at best $\ln s/s$. At the same time, the cross section for the simplest hard two-photon process, $e^+e^- \to e^+e^-q\bar{q}$ increases like $\ln^3 s$, for fixed transverse momentum of the quarks or fixed invariant mass of the $q\bar{q}$ pair. In fact, at high enough energies $\sqrt{s} \sim 1$ TeV, the combination of the increased cross section for resolved photon processes and the enhanced photon flux due to beamstrahlung can lead to severe hadronic backgrounds at e^+e^- supercolliders.

The photon content of electron is suppressed by $\alpha_{\rm em}$, but enhanced by a logarithmic factor $\sim \ln(s/4m_{\rm e}^2)$. In the kinematic regime of our interest ($\sqrt{s} > 300$ GeV), this means that an electron beam can be qualitatively visualized as carrying a photon beam with a flux $5 \sim 10\%$ that of the electron. Now, about a fraction $\alpha_{\rm em} \sim 10^{-2}$ of the time, we find a parton (quark or gluon) inside a photon. That is, taking all effects, electrons carry hadronic partons at the 10^{-3} level. If we consider double resolved processes, this means a factor of $10^{-3} \times 10^{-3} = 10^{-6}$ reduction in the flux. However, the parton diffractive scattering cross section is rather large, and it is essentially controlled by the cut-off in transverse momentum. This should be contrasted to the e^+e^- annihilation cross section, which is controlled by the total center-of-mass energy $\sqrt{s}$. While the annihilation cross section becomes very small at large $\sqrt{s}$, the diffractive cross section at fix transverse momentum cut increases with $\sqrt{s}$. Therefore, we would expect the resolved photon diffractive events to be produced at an reasonable level at future e^+e^- colliders, despite the flux reduction.

For the real $\gamma\gamma$ colliders, we expect cross sections much larger than the e^+e^- case, because the photons now are not coming from the electrons, hence there is less suppression of parton flux. (At high energies, such as is planned for the Next Linear Collider [17], potentially one should also consider W and Z bosons as partons inside electrons. But we will limit our scope here to the resolved photon contribution.)

For the resolved photon mechanism of generating jet events containing large rapidity gaps, we expect the spectator partons inside the photon to interact with the spectator

partons inside the opposite beam particle. That is, the situation is similar to the case of hadron-hadron collider. The soft spectator interaction can generate particles and spoil the rapidity gap. The rapidity survival probability $\langle S^2 \rangle$ is defined as the probability that no other interaction occurs beside the hard interaction of interest [2]. This probability is most readily estimated as an average over the hadron-hadron impact parameter B [2]:

$$\langle S^2 \rangle = \frac{\int d^2B f(B) S^2(B)}{\int d^2B f(B)}, \tag{1.1}$$

where $S^2(B)$ is the probability that the colliding hadrons do not interact inelastically, and $f(B)$ is the cross section for the hard collision of interest. Different estimates for $\langle S^2 \rangle$ in hadron collisions, based on a variety of phenomenological models, are presented in Ref. [18], where $\langle S^2 \rangle$ is estimated to be between 0.05 and 0.2. $\langle S^2 \rangle$ is expected to depend on the colliding energy, but only weakly on the size of the rapidity gap. In Ref. [19] the author uses a Good-Walker model for diffraction, and obtains a much higher value for the survival probability (44% at Tevatron energies, and 33% at 40 TeV.) On a related issue, the authors in Ref. [20] have used the HERWIG Monte Carlo program and found that in $\gamma\gamma$ and γp collisions, the mean number of hard interactions per event ranges from 1.04 to 1.123 for various particle colliders.

To obtain the cross section of jet events with rapidity gaps, we must multiply the hard collision cross section by the survival probability, that is,

$$\sigma_{\rm gap} = \langle S^2 \rangle \sigma_{\rm hard}. \tag{1.2}$$

Qualitatively, we expect the survival probability involving photon initial states to be approximately the same of the survival probability involving only hadronic initial states. This can be argued based on the vector meson dominance picture. However, it would be very interesting to study the difference of survival probabilities from hadronic and photonic initial states. The measurement of resolved photon gap events can clarify this difference.

In this paper we will present only the hard cross sections, without taking into the soft physics of the survival probability. But it will be implicitly understood that in order to obtain the final cross sections, the factor $\langle S^2 \rangle$ must be multiplied.

This paper is structured as follows. In Section II we will study the gap event cross section at HERA in the photon-proton double diffractive dissociation region. In Section III we analyze the situation at future linear collider energies (0.5 to 1.5 TeV), and in Section IV we analyze the situation for $\gamma\gamma$ colliders for a similar region of energies. Finally, in Section V we give the conclusions.

II. RESOLVED PHOTON GAP EVENTS AT HERA

The mechanism of generating resolved photon gap events at HERA *ep* collider is illustrated in Fig. 1. The partons that participate in the hard collision subprocess can be either quarks or gluons. We will consider the hard collision regime $|t| \gg 1$ GeV^2 where the perturbative pomeron is applicable. Notice that this kinematic regime differs from the previous gap event regimes in Ref. [5,6], where the proton remains unbroken or is excited to a low-mass state, and propagates down the beam pipe, escaping detection. That is, the rapidity gaps observed so far in HERA are between the real or virtual photon fragments and the unbroken proton or its excited state. This situation is different from the gap events observed at hadron-hadron colliders [4], where the rapidity gap is observed between two measured jets. Here in our paper, we consider a situation similar to the hadron-hadron collision case. That is, hard jets are generated both from the photon fragmentation and the proton fragmentation regions. This corresponds to the double diffractive dissociation of the γp system, and the rapidity gap exists between the two observed hard jets.

The diffractive scattering cross section for the quark-quark t-channel color-singlet exchange case has been obtained by Mueller and Tang [21] (see also Ref. [22]) by using the Balitsky-Fadin-Kuraev-Lipatov (BFKL) model [23]:

$$\frac{d\sigma_{qq}}{dt} = (\alpha_{\rm s} C_{\rm F})^4 \frac{\pi^3}{4t^2} \frac{e^{2(\alpha_{\rm P}-1)y}}{\left[\frac{7}{2}\alpha_{\rm s} C_{\rm A}\zeta(3) y\right]^3}, \tag{2.1}$$

where $\alpha_{\rm s} = \alpha_{\rm s}(-t)$ is the strong coupling constant, $y = \ln(-\hat{s}/t)$ is the rapidity interval between the two out-going partons as measured from the beam axis, where $\hat{s}$ is the total

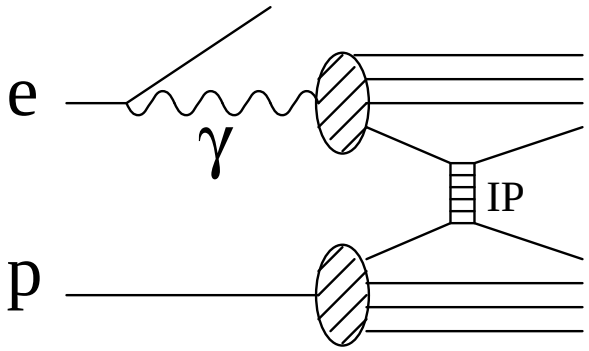

FIG. 1. Resolved photon mechanism for producing jet events with a large rapidity gap in ep collision. The partons inside the photon and the proton undergo a hard scattering via the exchange of a perturbative QCD pomeron.

center-of-mass energy squared of the qq system; $\alpha_{\rm P} = 1 + (4\alpha_{\rm s}C_{\rm A}/\pi)\ln 2$ the slope of the pomeron trajectory, $\zeta(3) = 1.20206\ldots$, and $C_{\rm A} = 3$ and $C_{\rm F} = 4/3$ the values of the Casimir operators in the adjoint and fundamental representations of the $SU(3)$ group. For the case of gluon-gluon elastic scattering with color-singlet t-channel exchange, we need only to replace the $C_{\rm F}$ factor in $d\sigma_{qq}/dt$ by $C_{\rm A}$. That is,

$$\frac{d\sigma_{gg}}{dt} = \alpha_{\rm s}C_{\rm A}\frac{\pi^3}{4t^2}\frac{e^{2(\alpha_{\rm P}-1)y}}{\left[\frac{7}{2}\zeta(3)y\right]^3}. \tag{2.2}$$

To obtain the total cross section, we must integrate the cross section of the hard collision weighed by the respective structure functions.

$$\begin{aligned}\sigma_{ep}(s, m^2_{\rm cut}, Y_{\rm cut}) = &\int_{(m^2_{\rm cut}, Y_{\rm cut})} dz dx_1\ dx_2\ dt\ f_{\gamma|e}(z,s) \\ &P_\gamma(x_1,-t)\ P_p(x_2,-t)\ \frac{d\sigma_{gg}}{dt}(\hat{s} = z x_1 x_2 s, t).\end{aligned} \tag{2.3}$$

In the above formula, z is the momentum fraction of the incoming electron carried by the photon, x_1 and x_2 are the momentum fraction of the partons carried by the photon and proton, respectively. $\sqrt{s}$ is the total center-of-mass energy of the ep system, $m^2_{\rm cut}$ is the minimum transverse momentum squared of the hard tagging jets, and $Y_{\rm cut}$ is the minimum rapidity interval separating the two hard jets. The number of photons carrying a fraction z of the energy of an emitting electron in leading log approximation is given by

$f_{\gamma|\mathrm{e}}(s,z) = \alpha_{\mathrm{em}}/(2\pi z)[1+(1-z)^2]\ln(s/4m_{\mathrm{e}}^2)$, with $\sqrt{s}$ the total center-of-mass energy of the colliding ep system and m_{e} the electron mass [10,24]. However, this formula overestimates the direct $\gamma\gamma \to q\bar{q}$ contribution [25]. An improved expression including non-leading terms is [26]:

$$f_{\gamma|\mathrm{e}}(z,s) = \frac{\alpha_{\mathrm{em}}}{2\pi z}\left\{ \left[1+(1-z)^2\right]\left(\ln(s/4m_{\mathrm{e}}^2)-1\right) + z^2\left[\ln\frac{2(1-z)}{z}+1\right] + (2-z)^2\ln\frac{2(1-z)}{2-z}\right\}, \tag{2.4}$$

This formula has been shown [25] to give accurate results not only for total (direct) jet rates but also for distributions. In Eq. (2.3), the quantities $P_\gamma(x_1,-t)$ and $P_p(x_2,-t)$ correspond to the parton structure functions of the photon and proton, respectively, and they are defined as

$$\begin{aligned} P_\gamma(x,Q^2) &= f_{g|\gamma}(x,Q^2) + \left(\frac{C_{\mathrm{F}}}{C_{\mathrm{A}}}\right)^2 \sum_q \Big[\, f_{q|\gamma}(x,Q^2) + f_{\bar{q}|\gamma}(x,Q^2)\,\Big], \\ P_p(x,Q^2) &= f_{g|p}(x,Q^2) + \left(\frac{C_{\mathrm{F}}}{C_{\mathrm{A}}}\right)^2 \sum_q \Big[\, f_{q|p}(x,Q^2) + f_{\bar{q}|p}(x,Q^2)\,\Big]. \end{aligned} \tag{2.5}$$

For the photon structure functions, we have the identity $f_{q|\gamma}(x,Q^2) = f_{\bar{q}|\gamma}(x,Q^2)$. There exist many parametrizations for the parton distributions inside proton and photon. For the photon distribution functions, we will limit ourselves to the Drees-Godbole (DG) parametrization [27] and to the Glück-Reya-Vogt (GRV-LO) parametrization [28]. (We thank the authors for providing the programs.) Numerically, the largest uncertainty in our calculation comes from the gluon density inside photon, where little experimental result is available. The quark densities are better understood. See the recent results by the TRISTAN's collaborations TOPAZ [29] and AMY [30] on the measurement of the photon structure function $F_2^\gamma(x,Q^2)$. It is worth mentioning that the gluon density of the photon in the GRV-LO parametrization is consistent with the recent measurement by the H1 Collaboration at HERA [31]. For the proton structure function, we choose the CTEQ 2'M parametrization from the CERN PDFLIB routine library [32]. We use $Q^2 = -t$ for the scale of the photon and proton structure functions.

We perform the numerical integration with the Monte Carlo integration program VEGAS [33]. The integration limits are

$$\begin{aligned} & 0 \leq z, x_1, x_2 \leq 1, \\ & m_{\rm cut}^2 \leq |t| \leq x_1 x_2 e^{-Y_{\rm cut}} s, \end{aligned} \tag{2.6}$$

where we integrate over all events with jet transverse momentum larger than $m_{\rm cut}^2$ and a rapidity separation between the jet centers larger than $Y_{\rm cut}$. It should be pointed out that due to the hadronization effect, the hadron fragments typically scatter around the jet centers, within a circle of radius ~ 0.7 units of rapidity [2]. Hence the observed effective gap is $Y_{\rm eff} \sim Y - 1.4$.

In Fig. 2 we present the result of the calculation. For $Y_{\rm cut} = 4$ and $m_{\rm cut} = 5$ GeV, even taken into account the survival probability consideration and uncertainty for the gluon distribution inside the photon, the gap events should still be produced at an observable rate. As we stated before, gap events have been observed at HERA both in the deep-inelastic regime [5] and in the photoproduction regime [6], where the rapidity gap exists between the photon (real or virtual) fragmentation region and the forward, undetected proton (or its excited state.) It would be interesting to verify the existence of rapidity gap between two observed hard jets at HERA, and study the dependence of these gap event cross sections on the rapidity interval $Y_{\rm cut}$ and on the transverse moment cut $m_{\rm cut}^2$, and compare with our calculation here. We should note, however, that smaller rapidity gaps can also arise from random fluctuation of the fragments of hadronization process. A systematic study of rapidity gap physics here and in other environments [4] will gradually allow better understanding of the relative importance of gap events from perturbative mechanisms and from random fluctuations, as well as insight to the survival probability involving photons.

It is important to point out, though, that our current knowledge of the photon structure functions is rather imprecise. This is especially true for the gluon content of photon, which numerically forms the dominant contribution to the gap event cross section. Therefore, an uncertainty of half an order of magnitude above or below the calculated curves would not be

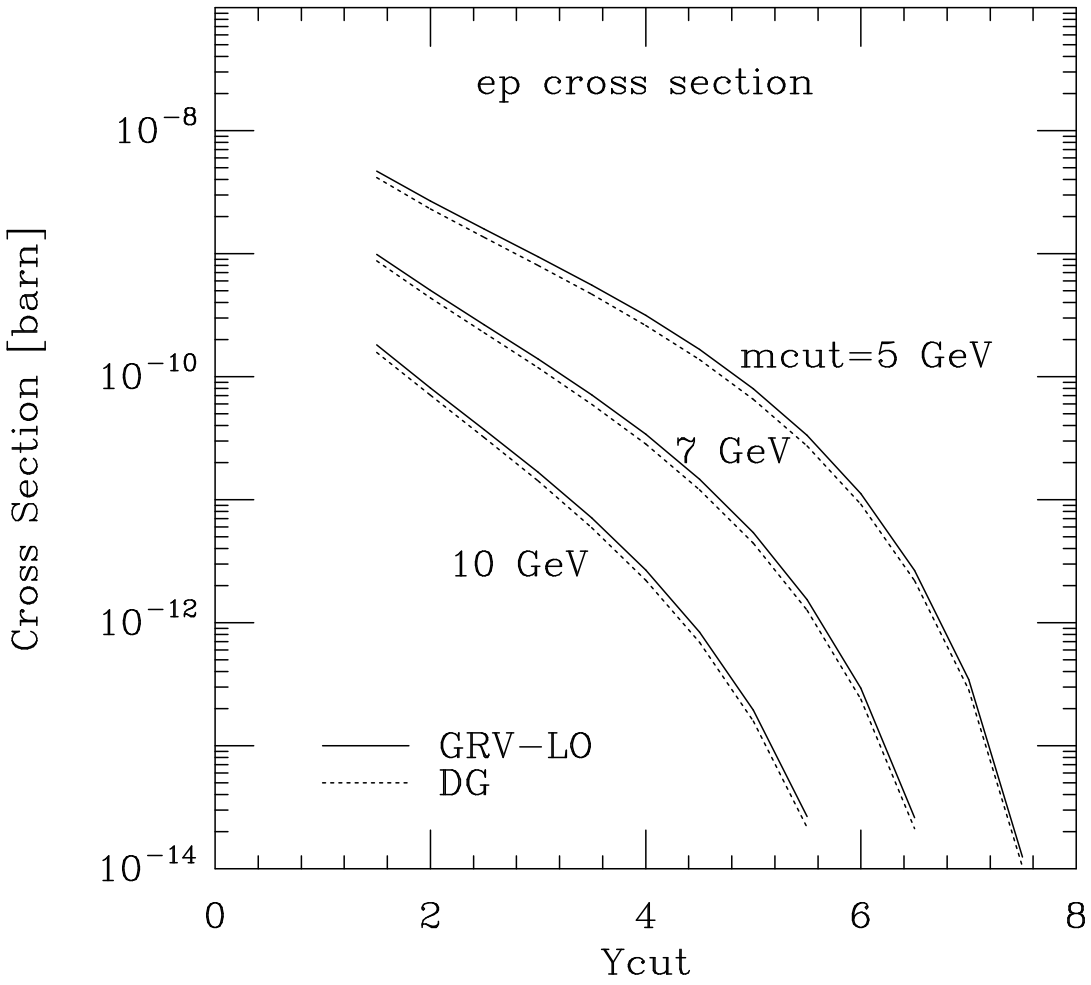

FIG. 2. Resolved photon gap event cross section at HERA, for various values of the transverse moment cut $m_{\rm cut}$. The solid lines are obtained with the Glück-Reya-Vogt parametrization of the photon structure functions, and the broken lines with the Drees-Godbole parametrization.

unreasonable. Hopefully the gluon content of the photon can be better measured at HERA in the future [31].

III. RESOLVED PHOTON GAP EVENTS AT NLC

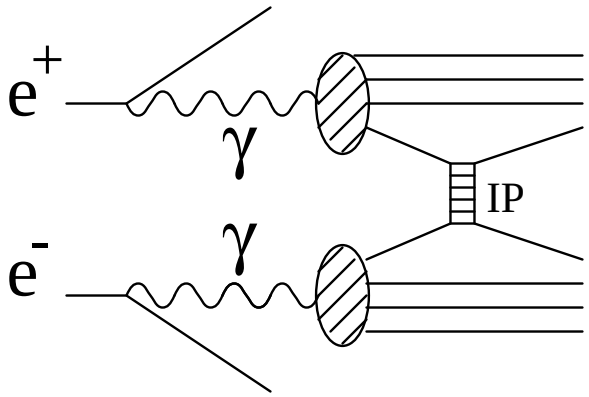

FIG. 3. Resolved photon mechanism for producing jet events with a large rapidity gap in e^+e^- collision. The partons inside the photons undergo a hard scattering via the exchange of a perturbative QCD pomeron.

The production mechanism is illustrated in Fig. 3. Currently, the energy projected for future e^+e^- colliders is in the range 0.5 to 1.5 TeV. At this energy range, the resolved photon contributions should be substantial. However, due to beamstrahlung background, the detectors for these colliders are not expected to be sensitive to jet production in the forward or backward direction. That is, many of the gap events will not be detected. We will analyze the production cross section of gap event by taking into account also the detector limitation. Here we will assume that the detector is only capable of observing hard jets produced in the rapidity region $[-\eta_{\rm det}, \eta_{\rm det}]$. Given this limitation, the observable rapidity gap events can be classified into three cases: (a) both hard jets are observed, (b) only the forward hard jet is observed, and (c) only the backward hard jet is observed. These situations are illustrated in Fig. 4. In the cases (b) and (c), since one of the hard jets is not measured, it is not possible to know the true size of the rapidity gap. For these cases, we define the empirical rapidity gap as the size of the rapidity interval between the hard jet and the detector limit on the

opposite side. Mathematically, if y_1 and y_2 represent the rapidities of the forward and the backward hard jet, then we define the empirical gap to be

$$Y = \mathrm{Min}\left\{y_1 - y_2, y_1 + \eta_{\rm det}, \eta_{\rm det} - y_2\right\}, \tag{3.1}$$

Naturally, the size of the rapidity gap cannot exceed the detector range: $Y < 2\eta_{\rm det}$.

To integrate the event cross section, we take into account the kinematic cuts from 1) detector limitation: $\eta_{\rm det}$, 2) rapidity gap cut: $Y_{\rm cut}$, and 3) transverse momentum cut: $m^2_{\rm cut}$.

$$\begin{aligned}\sigma_{e^+e^-}(s, m^2_{\rm cut}, Y_{\rm cut}, \eta_{\rm det}) = \int_{(m^2_{\rm cut}, Y_{\rm cut}, \eta_{\rm det})} & dz_1 dz_2 dx_1\ dx_2\ dt\ f_{\gamma|e}(z_1, s) f_{\gamma|e}(z_2, s) \\ & P_\gamma(x_1, -t)\ P_\gamma(x_2, -t)\ \frac{d\sigma_{gg}}{dt}(\hat{s} = z_1 z_2 x_1 x_2 s, t).\end{aligned} \tag{3.2}$$

The photon momentum fractions inside the electron and the positron are respectively z_1 and z_2. Other quantities that appear in this formula have been explained in the previous section. The integration momentum fractions are constrained to: $0 \le z_1, z_2, x_1, x_2 \le 1$. The gap and transverse momentum constraints impose the following limits for the t integration. For the case (a),

$$\mathrm{Max}\left\{\begin{array}{c} m^2_{\rm cut} \\ x_1^2 z_1 z_2 e^{-2\eta_{\rm det}} s \\ x_2^2 z_1 z_2 e^{-2\eta_{\rm det}} s \end{array}\right\} \ < \ |t| \ < \ x_1 x_2 z_1 z_2 e^{-Y_{\rm cut}} s. \tag{3.3}$$

For the case (b),

$$\mathrm{Max}\left\{\begin{array}{c} m^2_{\rm cut} \\ x_1^2 z_1 z_2 e^{-2\eta_{\rm det}} s \end{array}\right\} \ < \ |t| \ < \ \mathrm{Min}\left\{\begin{array}{c} x_1^2 z_1 z_2 e^{-2(Y_{\rm cut} - \eta_{\rm det})} s \\ x_2^2 z_1 z_2 e^{-\eta_{\rm det}} s \end{array}\right\}. \tag{3.4}$$

And for the case (c),

$$\mathrm{Max}\left\{\begin{array}{c} m^2_{\rm cut} \\ x_2^2 z_1 z_2 e^{-2\eta_{\rm det}} s \end{array}\right\} \ < \ |t| \ < \ \mathrm{Min}\left\{\begin{array}{c} x_1^2 z_1 z_2 e^{-\eta_{\rm det}} s \\ x_2^2 z_1 z_2 e^{-2(Y_{\rm cut} - \eta_{\rm det})} s \end{array}\right\}. \tag{3.5}$$

We include all three contributions in our integration of the event cross sections. In Fig. 5 and Fig. 6 are the results of the gap event cross sections, for 0.5 and 1.5 TeV center-of-mass

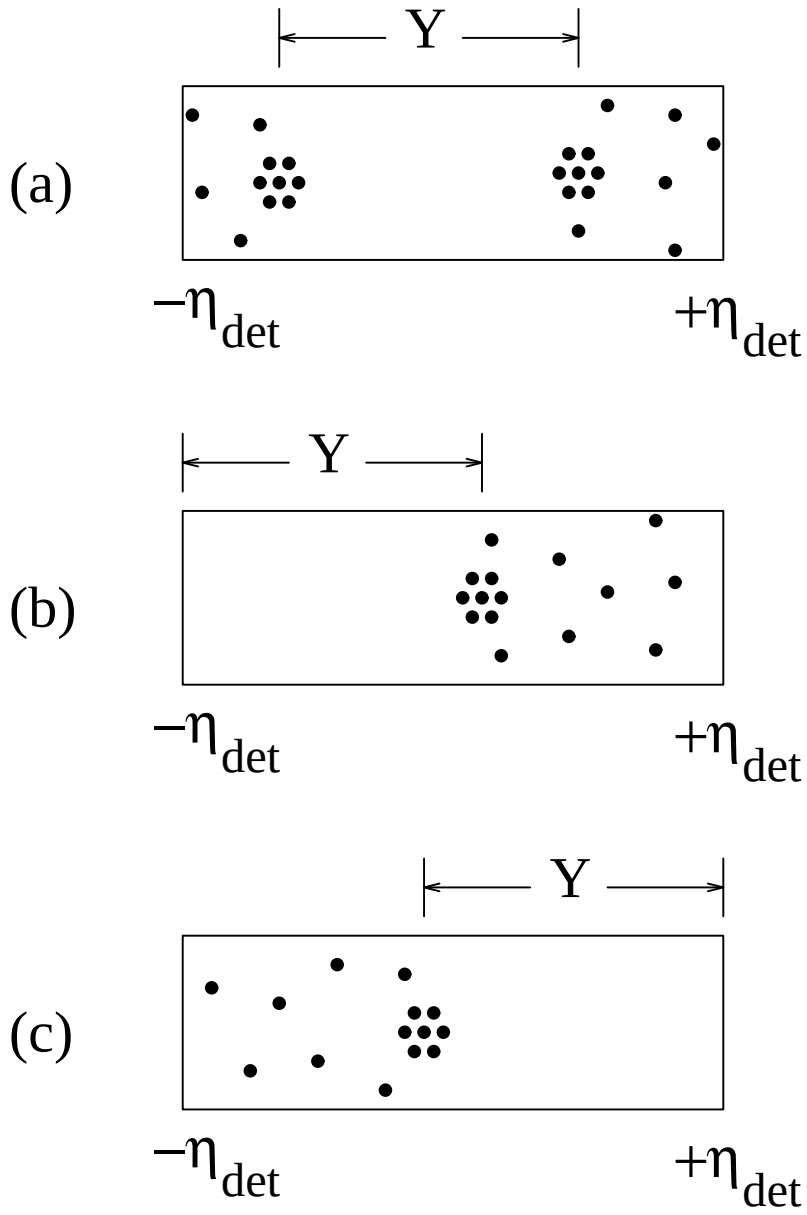

FIG. 4. Three possible cases for the observation of jet events containing rapidity gaps: (a) both hard jets are observed, (b) only the forward jet is observed, and (c) only the backward jet is observed. In the cases of (b) and (c), the gap size is measured from the jet center to the rapidity edge of the detector on the opposite side.

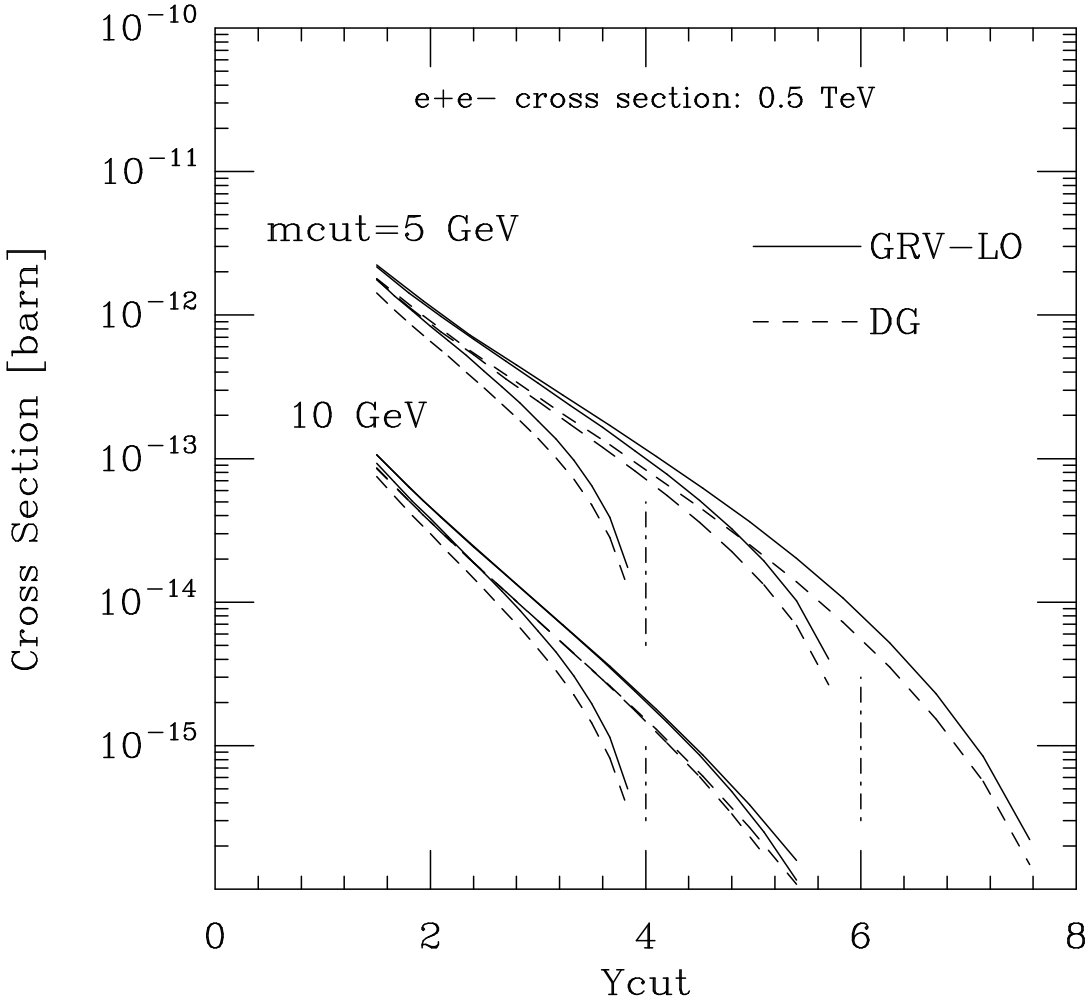

FIG. 5. Gap event cross section for e^+e^- collider at $E_{\rm cm} = 0.5$ TeV, for various values of transverse momentum cut $m_{\rm cut} = 5, 10$ GeV and detector rapidity limits $\eta_{\rm det} = 2, 3, 4$. The maximum observable rapidity gaps are $2\eta_{\rm det} = 4, 6, 8$ and are indicated by the dot-dashed vertical lines. The solid lines are obtained by using the Glück-Reya-Vogt parametrization of the photon structure functions, and the broken lines by using the Dree-Godbole parametrization.

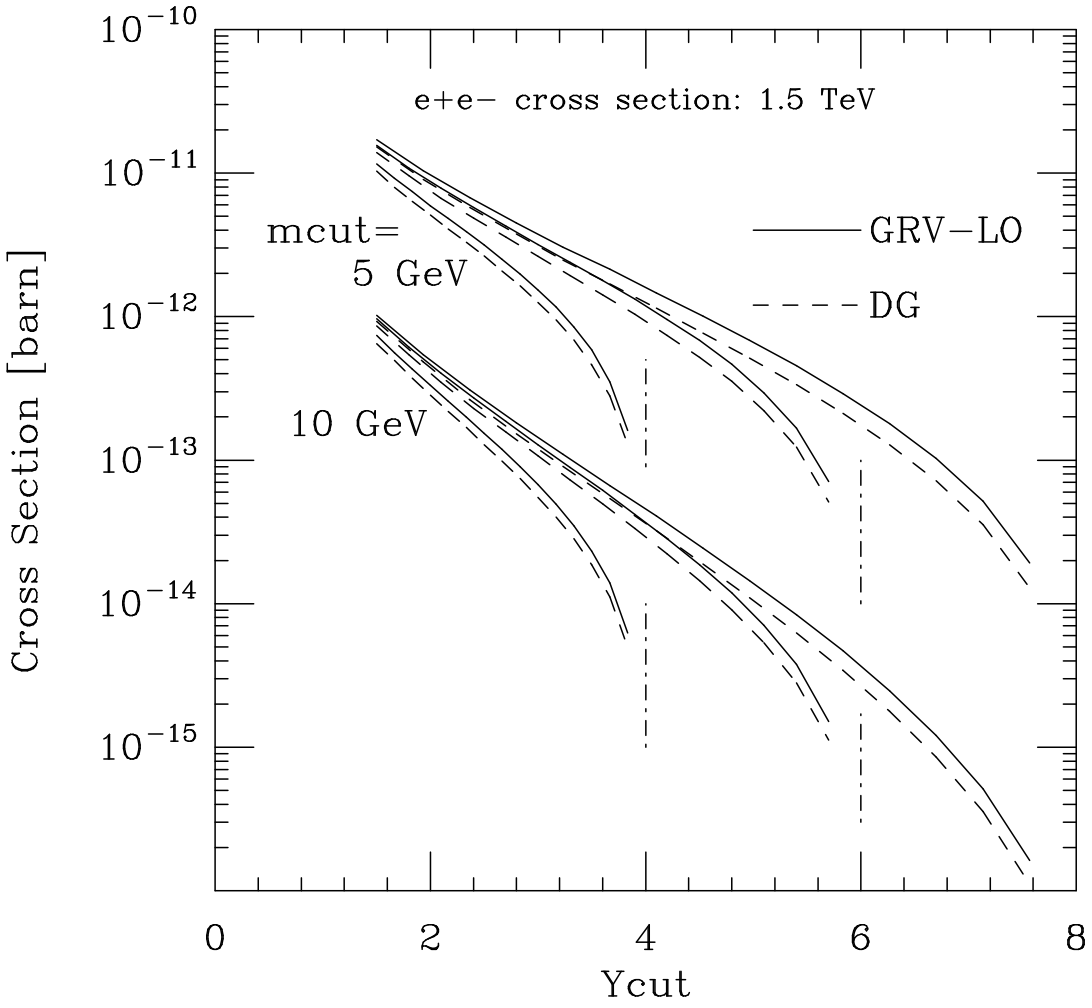

FIG. 6. Same as Fig. 5, but at a center-of-mass energy of $E_{\rm cm} = 1.5$ TeV.

energy. We consider three values for the maximum detector rapidity: $\eta_{\rm det} = 2, 3, 4$, which means that the maximum detectable rapidity gaps are respectively $Y = 4, 6, 8$. The curves are plotted for two values of the transverse momentum cut: $m_{\rm cut} = 5, 10$ GeV.

With the projected luminosity for the future linear colliders $\sim 10^{34}$ [cm^{-2}s^{-1}] , the detectors should be sensitive to the physics at cross section level of ~ 1 [fb]. Hence, unless the detector has very narrow range of rapidity, gap events with $Y_{\rm cut} = 4$ and $m_{\rm cut} = 5$ GeV should be produced at an observable rate, this even when the survival probability is taken into account. Notice that in going from 0.5 to 1.5 TeV, the gap event cross section increases by about an order of magnitude. (Naturally, we also have to keep in mind the uncertainty from the photon structure functions.)

In Ref. [8], various mechanisms for the production of rapidity gap events at LEP-II have been analyzed. These mechanisms can be characterized as the annihilation of e^+e^- into two gauge bosons, which subsequently decay into jet pairs. As opposed to the resolved photon mechanism studied here, in the annihilation mechanisms all the beam energy goes into the production of the hadronic jets. In principle, it is possible to distinguish these two mechanisms, by measuring the presence or absence of the e^+e^- in the forward or backward direction. (Calorimetry may also help, although the lepton colliders are not expected to be sensitive to forward and backward jets due to the background problems). In practice, this distinction may not always be feasible. In terms of orders of magnitude, the annihilation mechanisms like $e^+e^- \to \gamma^*\gamma^* \to jets$ and $e^+e^- \to \gamma^* Z \to jets$ may be produced at a competing level with the resolved photon cases (at least for the 0.5 TeV machine). Also, there are other mechanisms of producing gap events, such as coming from W and Z bosons, via annihilation or resolved mechanisms. In summary, there is a rich phenomenology still to be studied. We limit our scope here only to the resolved photon contribution, and postpone a more comprehensive analysis of rapidity gap jet events at NLC for the future.

IV. RESOLVED PHOTON GAP EVENTS AT $\gamma\gamma$ COLLIDER

As opposed to the e^+e^- case, there is no photon flux suppression for real photon collisions. Therefore, we expect the resolved photon events to provide a much larger cross section for gap events.

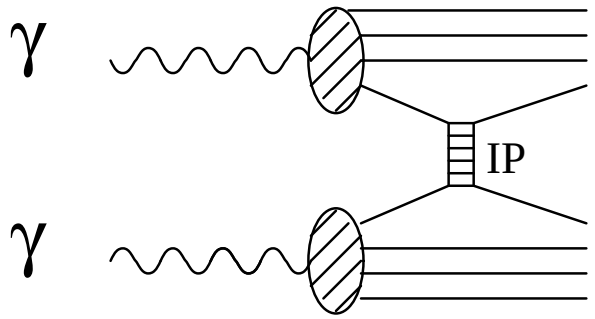

FIG. 7. Resolved photon mechanism for producing jet events with a large rapidity gap in $\gamma\gamma$ collision. The partons inside the photons undergo a hard scattering via the exchange of a perturbative QCD pomeron.

The production mechanism is illustrated in Fig. 7. As in the case of e^+e^- collider, we will assume a rapidity range of $[-\eta_{\rm det}, \eta_{\rm det}]$ for the detector. Although theoretically a $\gamma\gamma$ collider should have little beamstrahlung effects, hence the detectors should be able to observe jets near the forward and backward direction, in practice this may not be true. There remains serious technological challenge to the conversion of e^+e^- colliders into $\gamma\gamma$ colliders. In particular, the distance between the laser-backscattering points and the $\gamma\gamma$ collision point may not be large enough for the deflection of the remnant e^+e^- beams [34].

We also consider 0.5 to 1.5 TeV as the range for the center-of-mass energy. The event cross section is

$$\sigma_{\gamma\gamma}(s, m^2_{\rm cut}, Y_{\rm cut}, \eta_{\rm det}) = \int_{(m^2_{\rm cut}, Y_{\rm cut}, \eta_{\rm det})} dx_1\ dx_2\ dt\ P_\gamma(x_1, -t)\ P_\gamma(x_2, -t)\ \frac{d\sigma_{gg}}{dt}(\hat{s} = x_1 x_2 s, t). \tag{4.1}$$

And the integration limits for the t variable are similar to those ones given in Eq. (3.3), (3.4) and (3.5), upon substituting $z_1 = z_2 = 1$.

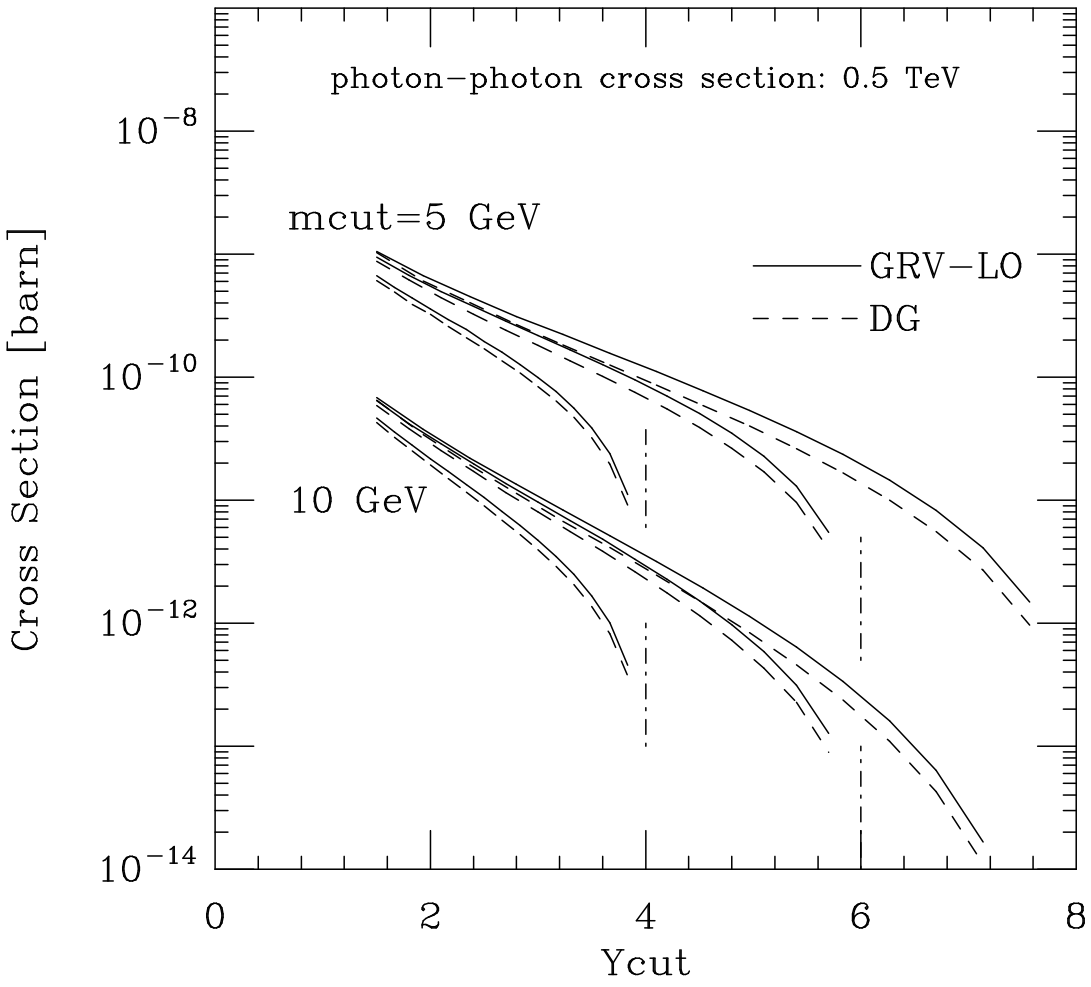

FIG. 8. Gap event cross section for $\gamma\gamma$ collider at $E_{\rm cm} = 0.5$ TeV, for various values of transverse momentum cut $m_{\rm cut} = 5, 10$ GeV and detector rapidity limits $\eta_{\rm det} = 2, 3, 4$. The maximum observable rapidity gaps are $2\eta_{\rm det} = 4, 6, 8$ and are indicated by the dot-dashed vertical lines. The solid lines are obtained by using the Glück-Reya-Vogt parametrization of the photon structure functions, and the broken lines by using the Dree-Godbole parametrization.

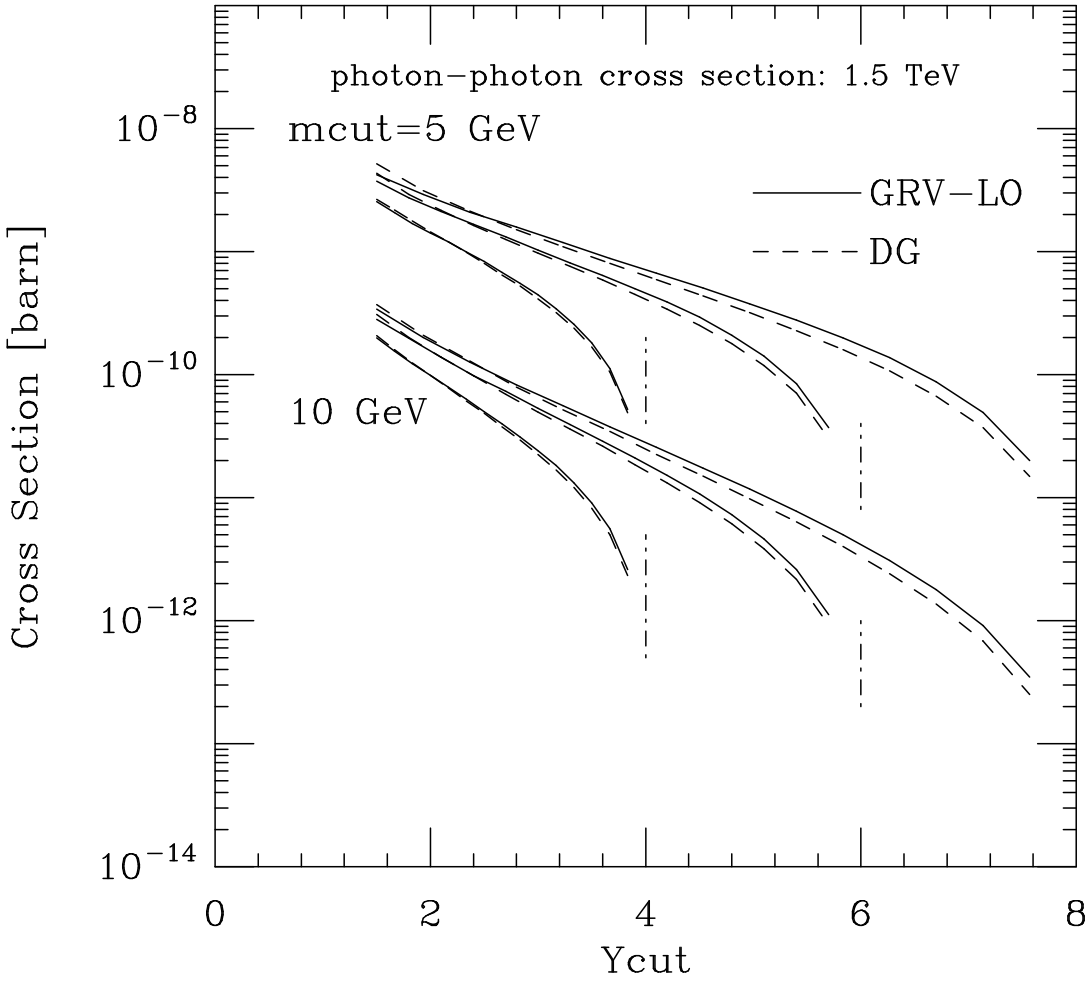

FIG. 9. Same as Fig. 8, but at a center-of-mass energy of $E_{\rm cm} = 1.5$ TeV.

The results for the cross sections are plotted in Fig. 8 and Fig. 9. We can see that compared to the e^+e^- case, the cross sections are now two to three orders of magnitude larger. Hence the gap events will be produced copiously at $\gamma\gamma$ colliders. This would provide the ideal environment of the study of survival probability involving photon initial states.

V. CONCLUSIONS

We have seen that resolved photons provides a mechanism of producing jet events containing large rapidity gaps, and we have analyzed the event cross section at HERA *ep* collider and future e^+e^- and $\gamma\gamma$ colliders. We have seen that in all three cases the event cross section are at the reach of the experiments. In the case of HERA, it would be interesting to observe the existence of rapidity gaps between two hard jet systems (one in the forward direction and the other one in the backward direction), and analyze the dependence of the cross section on the rapidity gap cut $Y_{\rm cut}$ and on the transverse momentum cut $m_{\rm cut}$. This would provide a first look into the survival probability involving photon-hadron collision. In the case of $\gamma\gamma$ collision we have seen that the event cross section becomes two to three orders of magnitude larger than the e^+e^- case. We have also seen that the resolved photon gap events increase significantly with the total center-of-mass energy. The observation of these events will allow the study of the perturbative QCD pomeron physics in environments alternative to the hadron-hadron colliders, provide insight into the survival probability physics of photons, and also allow further understanding on the relative importance of gap events coming from random fluctuation of hadronization effects and from perturbative mechanisms.

We very especially thank Wai-Keung Tang, for all the help received during the preparation of this work. We also thank Ina Sarcevic, Stanley Brodsky and Clemens A. Heusch for helpful conversations, and M. Drees, M. Glück, E. Reya and A. Vogt for providing the subroutines for the photon structure functions.

This work was supported by U.S. Department of Energy Grants No. DE–FG03–93ER40792.

REFERENCES

[1] J. D. Bjorken, Phys. Rev. D 45, 177 (1992).

[2] J. D. Bjorken, Phys. Rev. D 47, 101 (1992).

[3] Yu. L. Dokshitzer, V. A. Khoze and S. I. Troyan, in: Proc Sixth Intern. Conf. on Physics in Collision (1986), ed. M. Derrick (World Scientific, Singapore, 1987) p. 417; Yu. L. Dokshitzer, V. A. Khoze and T. Sjöstrand, Phys. Lett. B 274, 116 (1992).

[4] D0 Collaboration (S. Abachi et al.), Phys. Rev. Lett. 72, 2332 (1994); CDF Collaboration (F. Abe et al.), Phys. Rev. Lett. 74, 855 (1995).

[5] ZEUS Collaboration (M. Derrick et al.), Phys. Lett. B 315, 481 (1993), Phys. Lett. B 332, 228 (1994); H1 Collaboration (T. Ahmed et al.), Nucl. Phys. B 429, 477 (1994).

[6] ZEUS Collaboration (M. Derrick et al.), Phys. Lett. B 346, 399 (1995), preprint DESY-95-115; H1 Collaboration (T. Ahmed et al.), Nucl. Phys. B 435, 3 (1995).

[7] J. Randa, Phys. Rev. D 21, 1795 (1980); J. D. Bjorken, S. J. Brodsky and H. J. Lu, Phys. Lett. B 286, 153 (1992); H. J. Lu, S. J. Brodsky and V. A. Khoze, Phys. Lett. B 312, 215 (1993); J. Ellis and D. A. Ross, preprint CERN-TH-95-84.

[8] H. J. Lu, Nucl. Phys. B 427, 455 (1994).

[9] I. Ginzburg, G. Kotkin, S. Panfil, V. Telnov, Pizma ZhETF 34, 514 (1981); JETP Lett. 34, 491 (1982).

[10] C. F. Weisäcker, Z. Phyr. 88, 612 (1934); E. J. Williams, Phys. Rev. 45, 729 (1934).

[11] G. Ingelman and P. Schlein, Phys. Lett. B 152, 256 (1985); A. Donnachie and P. V. Landshoff, Nucl. Phys. B 303, 634 (1988), Phys. Lett. B 285, 172 (1992); H. J. Lu and J. Milana, Phys. Lett. B 313, 234 (1993); A. Edin, G. Ingelman and J. Rathsman, preprint DESY-95-145.

[12] E. Witten, Nucl. Phys. B 120, 189 (1979).

[13] C. H. Llewellyn Smith, Phys. Lett. B 79, 83 (1979).

[14] S. J. Brodsky, T. A. DeGrand, J. F. Gunion and J. Weis, Phys. Rev. Lett. 41, 672 (1978), Phy. Rev. D 19, 1418 (1979); K. Kajantie and R. Raitio, Nucl. Phys. B 159, 528 (1979); S. P. Li and H. C. Liu, Phys. Lett. B 143, 489 (1984).

[15] M. Drees and R. M. Godbole, Pramana J. Phys. 41 (1993) 83.

[16] M. Drees and R. M. Godbole, Z. Phys. C59, 591 (1993).

[17] F. A. Harris, S.L. Olsen, S. Pakvasa and X. Tata, editors, Workshop on Physics and experiments with linear e^+e^- colliders, Waikoloa, 1993.

[18] E. Gotsman, E.M. Levin and U. Maor Phys. Lett. B 309, 199 (1993).

[19] R. S. Fletcher, Phys. Lett. B 320, 373 (1994).

[20] J. M Butterworth, J. R. Forshaw, M. H. Seymour, J. K. Storrow and R. Walker, preprint CERN-TH/95-83.

[21] A.H. Mueller and W.-K. Tang, Phys. Lett. B 284, 123 (1992).

[22] A.H. Mueller and H. Navelet, Nucl. Phys. B 282, 727 (1987); V. Del Duca, M.E. Peskin and W.-K. Tang, Phys. Lett. B 306, 151 (1993); V. Del Duca and W.-K. Tang, Phys. Lett. B 312, 225 (1993); V. Del Duca, talk given at 10th Topical Workshop on Proton-Antiproton Collider Physics.

[23] E. A. Kuraev, L. N. Lipatov and V. S. Fadin, Sov. Phys. JETP 44, 443 (1976), *ibid.* 45, 199 (1977); Ya. Ya. Balitsky and L. N. Lipatov, Sov. J. Nucl. Phys. 28, 822 (1978); L, N. Lipatov, Sov. Phys. JETP 63, 904 (1986); V. Del Duca, report DESY-95-023; E. Levin, report CBPF-NF-010/95.

[24] A. C. Bawa and W. J. Stirling, J. Phys. G 15, 1339 (1989).

[25] R. Bhattacharya, J. Smith and G. Grammer, Jr. Phys. Rev. D15, 3267 (1977).

[26] S. J. Brodsky, T. Kinoshita and H. Terazawa, Phys. Rev. D4, 1532, (1971).

[27] M. Drees and R.M. Godbole, Z. Phys. C 28, 451 (1985).

[28] M. Glück, E. Reya and A. Vogt, Phys. Rev. D 45, 3986 (1992); Phys. Rev. D 46, 1973 (1992).

[29] TOPAZ Collaboration, K. Muramatsu *et. al*, Phys. Lett. B 332, 477 (1994).

[30] AMY Collaboration, S. K. Sahu *et. al*, Phys. Lett. B 346, 208 (1995).

[31] H1 Collaboration, Report DESY-95-062 (1995).

[32] H. Plothow-Besch, Comput. Phys. Commun. 75, 396 (1993).

[33] G.P. Lepage, J. Comput. Phys. 27, 192 (1978).

[34] C. A. Heusch, private communication.